

1 Exploiting the signal to noise ratio in multi-system predictions 2 of boreal summer precipitation and temperature

3
4 **Juan C. Acosta Navarro¹ and Andrea Toreti¹**

5 ¹European Commission, Joint Research Centre, Ispra, Italy.

6 *Correspondence to:* Juan C Acosta Navarro (juan.acosta-navarro@ec.europa.eu)

7 8 **Abstract**

9
10 Droughts and heat-waves are among the most impactful climate extremes. Their co-occurrence can have adverse
11 consequences on natural and human systems. Early information on their possible occurrence on seasonal
12 timescales is beneficial for many stakeholders. Seasonal climate forecasts have become openly available to the
13 community but a wider use is currently hindered by limited skill in certain regions and seasons. Here we show
14 that a simple forecast metric from a multi-system ensemble, the signal to noise ratio, can help overcome some
15 limitations. Forecasts of mean daily near surface air temperature and precipitation in boreal summers with high
16 signal to noise ratio tend to coincide with observed larger deviations from the mean than summers with small
17 signal to noise ratio. The signal to noise ratio of the ensemble predictions [may](#) serve as a complementary measure
18 of forecast reliability that could [potentially](#) benefit users of climate predictions.

19 20 **1. Introduction**

21
22 Droughts are typically slow onset climate extreme events (Mishra and Singh, 2010), yet they can be disruptive
23 and affect millions of people every year (Below et al., 2007; Enekel et al., 2020). Heat-waves can intensify and
24 trigger a faster drought evolution (Bevacqua et al., 2022). Compound drought and heat-waves can strongly impact
25 socio-economic and ecological systems, and may even compromise our ability to reach the UN sustainable
26 development goal on climate action while strongly reducing the Earth system's current natural capacity to absorb
27 and store carbon (Yin et al., 2023). The use of seasonal climate forecasts can provide actionable information to
28 reduce the risks and the impacts of these events on key sectors like agriculture, energy, transport, water supply
29 (Buontempo et al 2018; Ceglar and Toreti 2021).

30
31 In the last couple of decades, climate predictions have shown important progress in anticipating the evolution of
32 various components of the climate system across the subseasonal to decadal time range (Merryfield et al., 2020;
33 Meehl et al., 2021). A combination of multiple forecast systems has shown overall benefits as compared with
34 single systems, and can improve forecast quality up to a certain extent (Hagedorn et al., 2005; Mishra et al., 2019).
35 In spite of the recent progress, climate predictions still exhibit low to moderate skill in many regions and seasons
36 (e.g. European summer; Mishra et al. 2019), something that limits their use and represents a barrier for
37 stakeholders. Furthermore, multiple studies have shown that large ensembles are required to achieve skillful
38 predictions, something that seems to be related to the forecast systems being more skillful at predicting real climate

39 than at predicting their own realizations (i.e. ensemble members). This odd phenomenon has been called the signal
40 to noise paradox (Eade et al., 2014; Scaife and Smith, 2018; Smith et al., 2020). It is particularly evident in the
41 Euro Atlantic region during winter both on seasonal and decadal timescales. However boreal summer predictions
42 have been generally overlooked. A recent study based on a single forecasting system has shown that sampling
43 years with high SNR results in more skillful predictions of monthly temperatures in Japan throughout the year
44 (Doi et al., 2022).

45
46 In this study we exploit multi-system ensembles to test whether specific boreal summers with higher than normal
47 predictability can be detected through the local relation between skill and SNR. We explore this for near surface
48 air temperature and precipitation ~~predictions~~, both locally and on large aggregated mid-latitude regions of the
49 Northern Hemisphere.

50 51 **2. Methods**

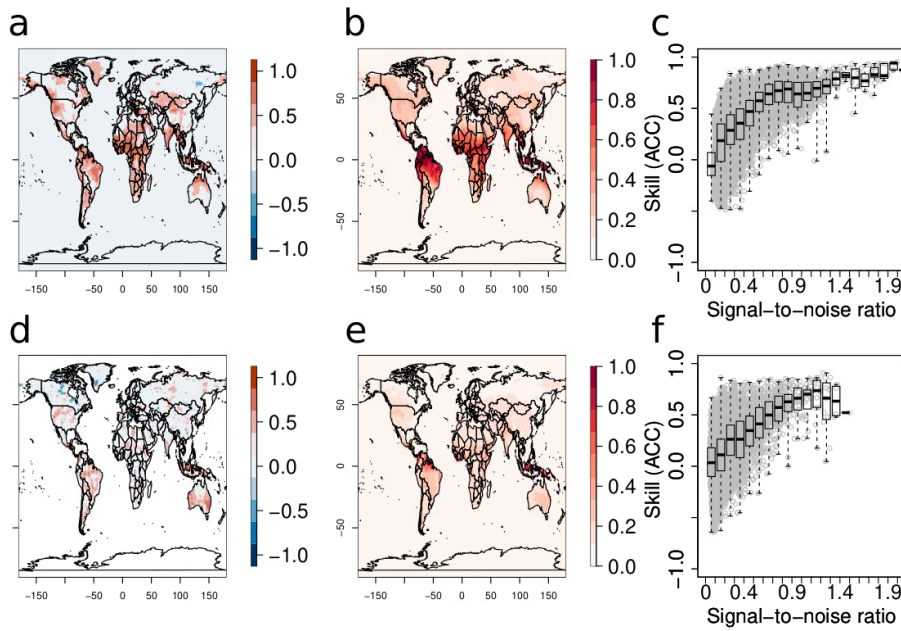
52
53 This analysis is based on seasonal re-forecasts (also known as hindcasts) of mean boreal summer precipitation
54 and 2-meter mean daily temperature (T2m) for the period 1993-2016 from ECMWF SEAS5 (S5, Johnson et al.,
55 2019), UKMO GloSea6 (S600, MacLachlan et al., 2015), MeteoFrance (S8, Batté et al., 2021), CMCC (S35,
56 Gualdi et al., 2020) and DWD (S21, Baehr et al., 2015), available from the Copernicus C3S Climate Data Store.
57 The observationally based datasets to evaluate the re-forecasts are ERA5 (Hersbach et al., 2020) for T2m and GPCC
58 (Schnider et al., 2011) for precipitation. The use of summer mean T2m is not intended to characterize single heat
59 waves, but to estimate average daily deviations from the mean on a seasonal scale. In a climatological sense, more
60 intense, more frequent or longer heat-waves than usual generally define hot summers and hence average T2m may
61 be seen as a seasonal integrator of heat-wave activity. Forecast skill is evaluated with the anomaly correlation
62 coefficient (ACC) between the ensemble mean and the observational reference. To complement the skill estimates
63 of ACC, two additional deterministic skill metrics are computed: the mean squared skill score (MSSS, Murphy,
64 1988) and the Gilbert skill score (GSS, WMO, 2014). The mean squared skill score compares the mean square
65 error of the forecasts with the mean square error of the climatological value. It ranges from minus infinity to 1
66 and values above 0 indicate skill in the predictions. The GSS measures the fraction of correctly predicted events
67 over the total number of predicted events plus misses, and takes into consideration the randomly predicted events.
68 The thresholds to define event/non event are the top and bottom 25% summers for T2m (hot) and precipitation
69 (dry), respectively. Standardization of the anomalies of each ensemble member and the observational reference
70 data is performed prior to the analysis. This step guarantees that each member from each system has a comparable
71 year-to-year variability to the observed one. Additionally, the standardized T2m anomalies are linearly detrended
72 at the grid level and for each member of the re-forecasts and in ERA5 to isolate as much as possible the impact of
73 the long term warming.

74
75 Following Doi et al. (2022), the SNR is calculated as: $SNR = \frac{\mu_e}{\sigma_e}$, where μ_e is the multi-system ensemble mean
76 and σ_e is the multi-system standard deviation after standardization, computed across ensemble members for every
77 summer (June - August) and for each gridbox. 25 members per system are used to have an equal contribution from
78 each system.

79
80
81
82
83
84
85
86
87
88
89
90
91

3. Signal to noise ratio and forecast skill

Figure 1 displays spatial maps of mean (boreal) summer T2m ACC, time averaged SNR, and a scatter plot which shows the local relation between ACC and SNR. On average, skill values over land increase with higher SNR values. Negative values of ACC are nearly non-existent when the threshold of SNR exceeds the value of about 0.5 in the same gridbox. Statistically significant skill in T2m is mostly confined to the tropics and sub-tropics. However, significant skill is also found in western North America, the eastern Mediterranean, central Asia and southern South America. Notable exceptions in the tropics are Congo and parts of the Amazon rainforests. The patterns of SNR largely mirror those of ACC. Generally, there is a good agreement between areas of high skill (ACC) and areas with high SNR, something that is further confirmed by the local relation between ACC and SNR (Fig. 1c).

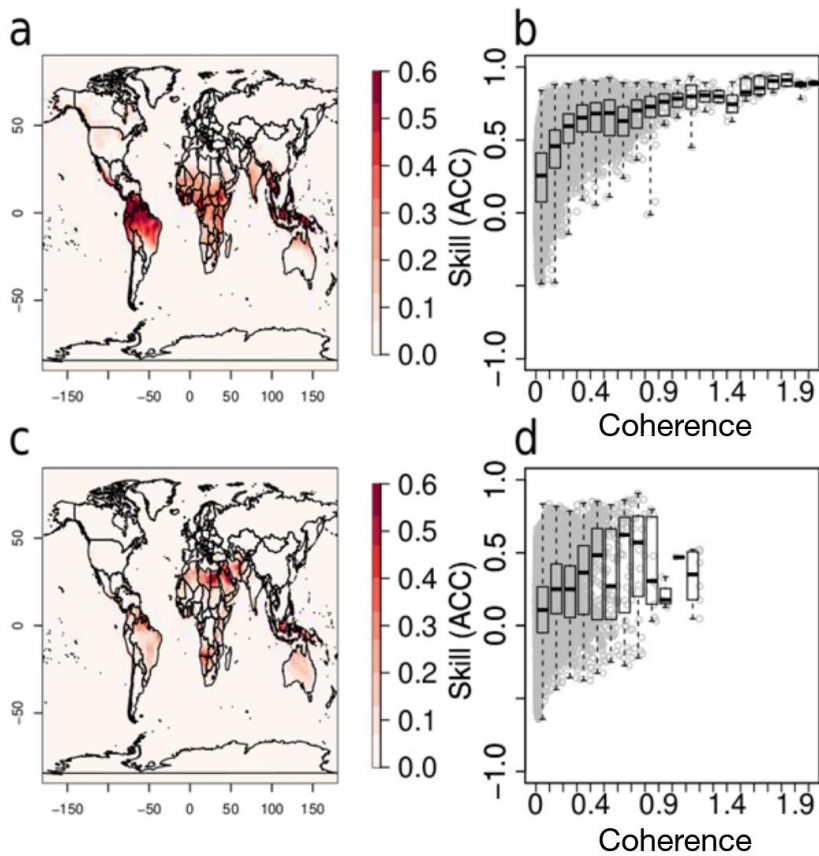


92
93
94
95
96
97
98
99
100

Figure 1: June-August Skill (ACC), time averaged SNR and scatterplots of local relation between ACC and SNR for T2m (a-c) and precipitation (d-f). Each gray dot in c,f represents the values of ACC and SNR at each gridbox. Only statistically significant values with a 90% confidence based on a t-test are displayed in (a,d). The re-forecasts are initialized every May.

Precipitation follows a similar behavior in terms of ACC and SNR, although statistically significant skill is less widespread (Fig. 1d-f). Areas under the influence of El Niño Southern Oscillation (ENSO; Lenssen et al., 2020) appear as regions with significant ACC and high SNR. Skillful values are mostly located in the Americas, the

101 Maritime continent and Australia. Precipitation skill and SNR in Africa and Asia are much lower, making these
 102 the regions with the largest qualitative differences between the two variables.
 103

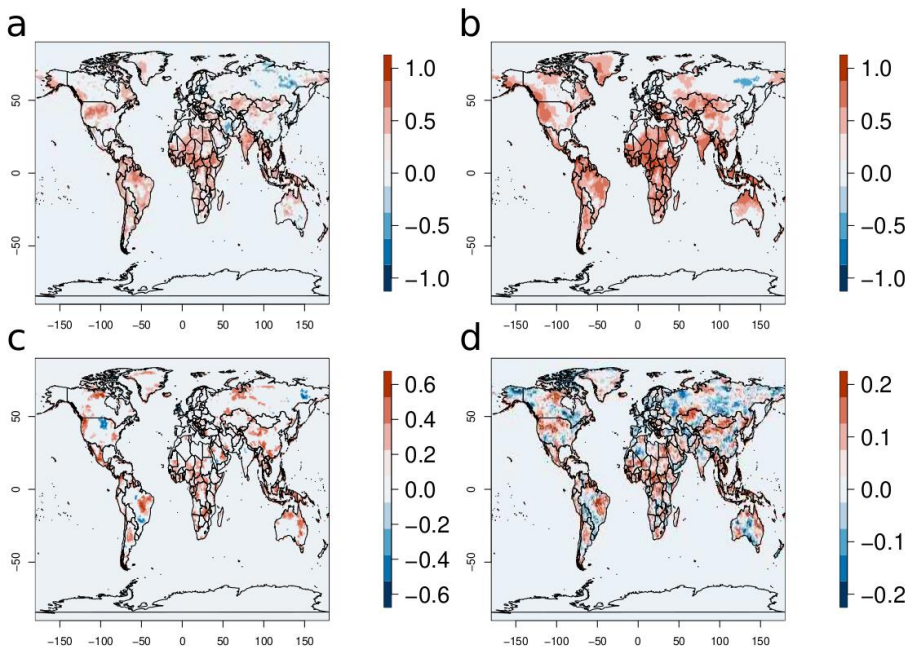


104
 105 **Figure 2: June-August time averaged ensemble coherence ($= \frac{\mu}{\sigma_e} - 1$) and scatterplots of the local relation between ACC**
 106 **and ensemble coherence for T2m (a-b) and precipitation (c-d). Each gray dot in b,d represents the values of ACC and**
 107 **ensemble coherence at each gridbox. The re-forecasts are initialized every May.**

108
 109 In Figure 2 we show the effect of the ensemble coherence on skill. Ensemble coherence is defined as the inverse
 110 of the ensemble standard deviation (σ_e), minus one. The spatial distribution of time averaged ensemble coherence
 111 displays many similarities to the SNR for both T2m and precipitation, although the signal is clearly dominated by
 112 the tropics and subtropics with virtually no contribution from the extra-tropics, except for a minor one from T2m
 113 in western North America and from precipitation in the Middle East (Fig. 2a,c). In terms of the local relation
 114 between ensemble coherence and skill, T2m displays a clear increase in skill with higher values of coherence (Fig.
 115 2b). Skill is virtually always positive when coherence values exceed 0.3, implying that ensemble spread may also
 116 be a good indicator of skill for T2m, similar to SNR. For precipitation there is weaker relation between skill and

117 ensemble coherence than for T2m as there appear to be as many locations of high coherence with little skill as
118 there are locations with high skill and high coherence (Fig. 2d). This can be a result of a weaker relation between
119 skill and ensemble coherence than between skill and SNR, but may also be at least partially a result of the large
120 uncertainty in observed precipitation in many regions.

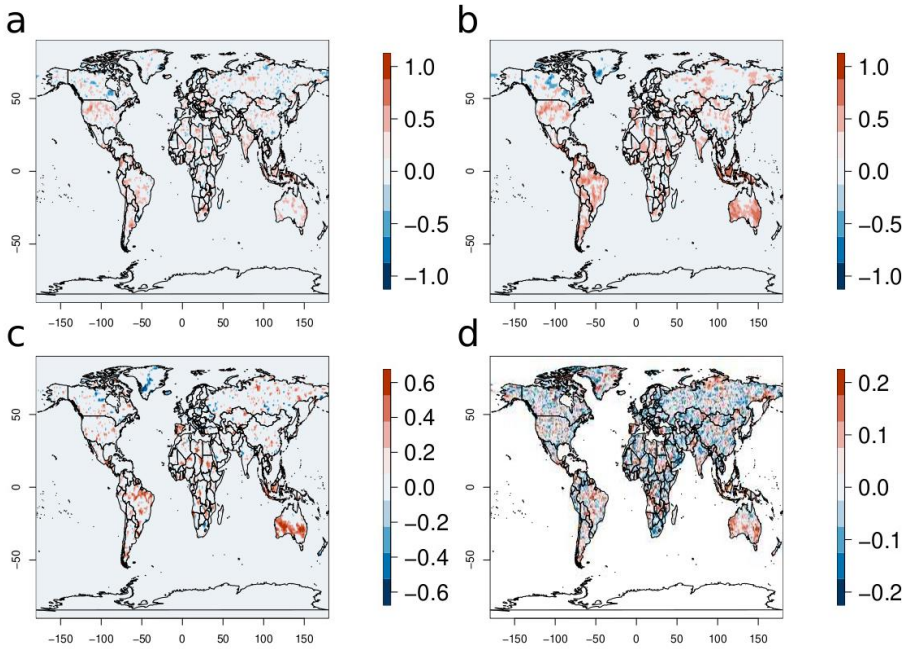
121
122 Based on the observed link between skill and SNR, we use the latter one as the single criterion to exclude from
123 the re-forecasts years with very low and very high values to understand their impact on skill. When 25% of the
124 years (6 in total) with the highest SNR (Fig. 2Fig. 3a) are excluded, the results overall show much lower values
125 of ACC than when only 25% of the years with the lowest SNR are excluded (Fig. 2Fig. 3b). Furthermore,
126 differences between the latter and the former result (in many cases) in higher statistically significant values than
127 the ACC computed when selecting only years without the highest SNR (Fig. 2Fig. 3a,c). This result highlights the
128 importance that these extreme SNR years can have on skill. In fact, only skill values that are computed by
129 excluding the bottom 25% of SNR years (Fig. 2Fig. 3b) are comparable to the ones estimated when all years are
130 used for the computation (Fig. 1a).



132
133 **Figure 3:** Skill (ACC) of T2m predictions excluding 25% of the years with highest (a) and lowest (b) local SNR. (c)
134 **Difference between (a) and (b).** (d) **Difference in the time-averaged absolute deviation from the mean in ERA5 T2m,**
135 **excluding years having 25% of the lowest and highest local SNR, respectively. Only statistically significant values with**
136 **a 90% confidence based on a t-test are displayed in (a-c). The re-forecasts are initialized every May.**

137
138 Interestingly, using the same criterion to select ERA5 T2m values reveals that in general, excluding years with
139 high ensemble SNR results in lower absolute deviations from the mean than when the low SNR years are excluded

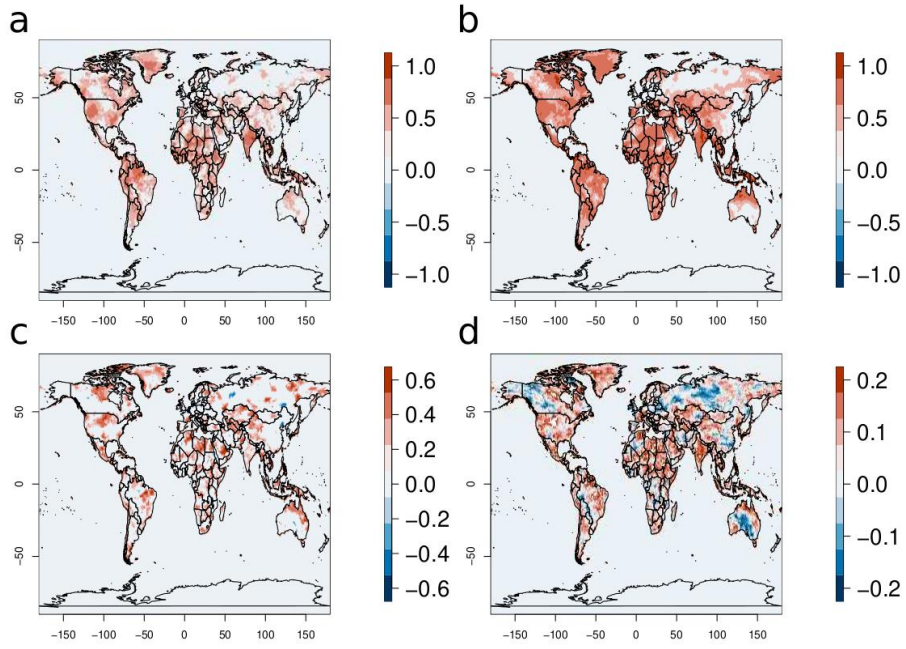
140 (Fig-2Fig. 3d). Additionally, these differences overall coincide with regions with significant skill differences (Fig-
 141 2Fig. 3c,d). This implies that years with more extreme deviations from the mean (in the observations/reanalysis)
 142 may be identified a priori by calculating the ensemble SNR of the forecast, and that forecast systems are in general
 143 more skillful when large deviations from the mean occur.
 144



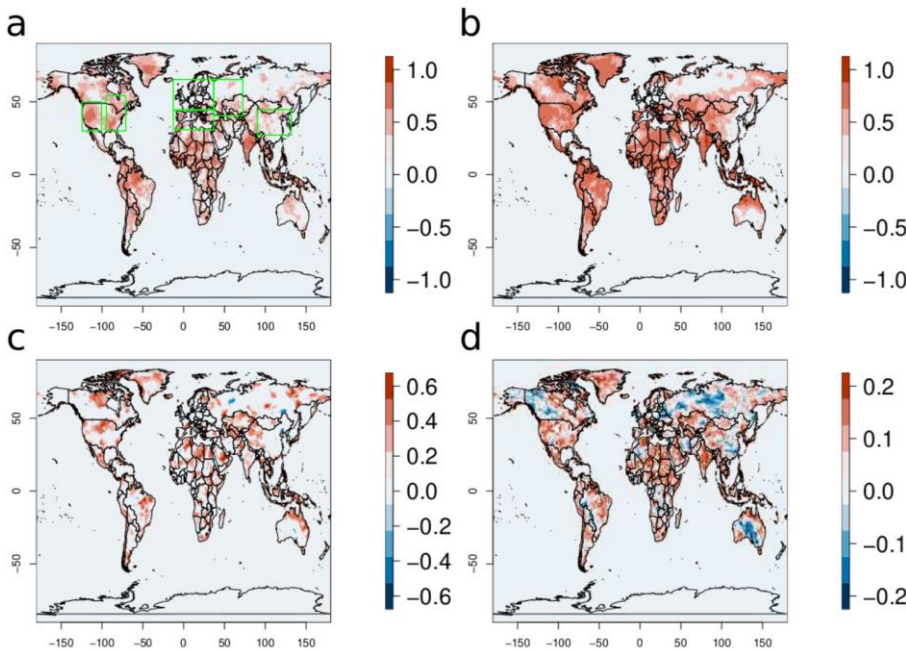
145
 146 **Figure 43:** Same as Figure 32, but for precipitation.
 147

148 Similar to T2m, the exclusion of years with high SNR also results in lower overall precipitation skill values than
 149 the one obtained when excluding low SNR years (Fig-3Fig. 4a,b). Important skill differences appear in the Iberian
 150 Peninsula, Brazil, Australia and Indonesia (Fig-3Fig. 4c), and in most cases imply a shift from non-significant to
 151 significant skill (Fig-3Fig. 4 a and b, respectively). Contrasting with T2m, the relation between ACC and mean
 152 absolute deviation from the mean in the observations is not obvious for precipitation (Fig-3Fig. 4c,d). To further
 153 investigate this behavior, we analyzed the relationship between skill differences and the differences in absolute
 154 deviation from the mean for T2m and precipitation, as usual by using the re-forecasts that exclude the 25% of the
 155 years with the lowest and the highest SNR, respectively. This analysis (not shown) confirms a statistically robust
 156 relationship between skill and large deviations from mean observed precipitation, but still weaker than for T2m.
 157

158



159



160

Figure 54: The same as Figure 32, but for re-forecasts initialized every June. **Boxes in (a) show the areas used in Figures 6 and 7.**

161

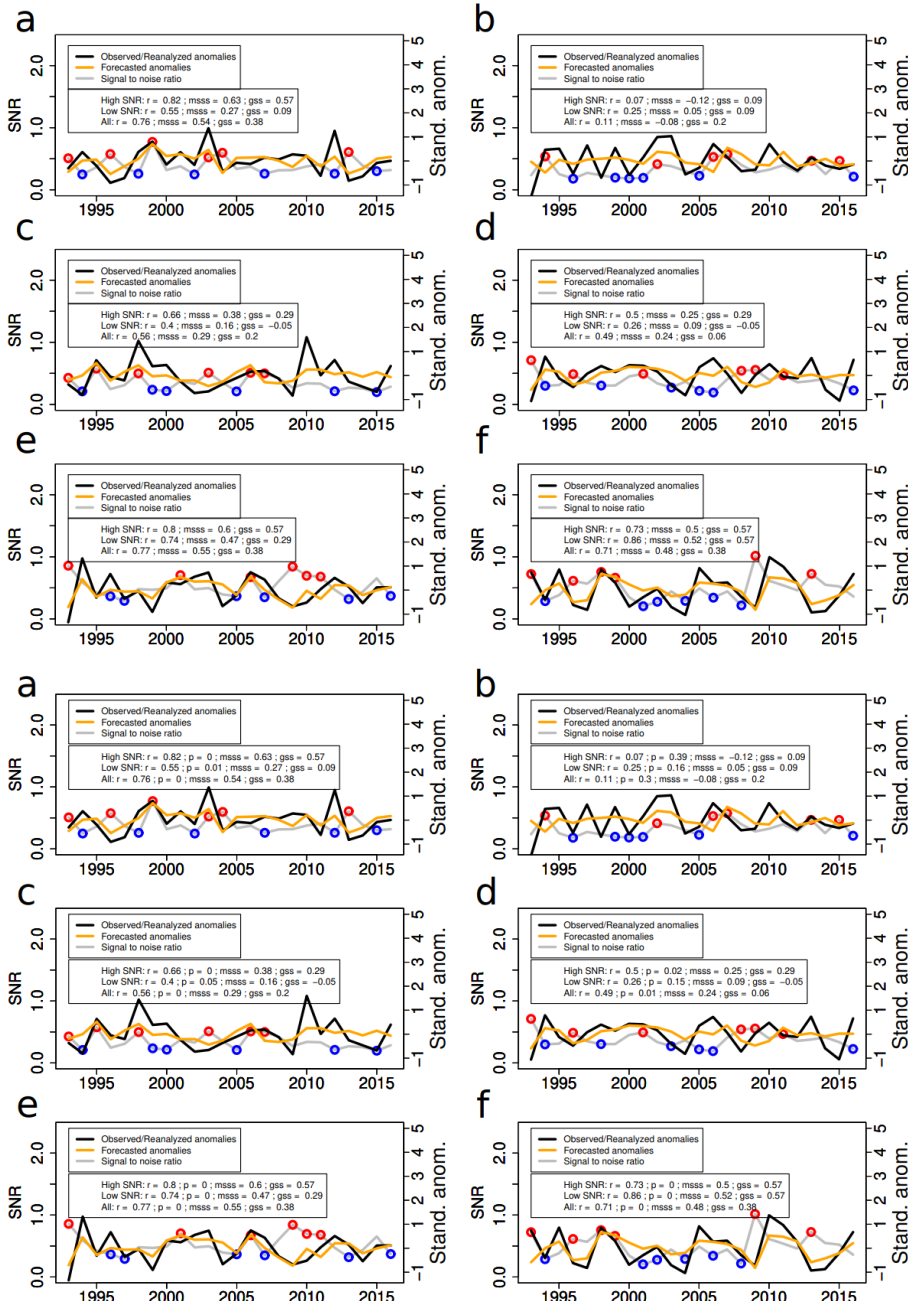
162
163 Figure 54 shows a clearer relation between the impact on skill of the most extreme years in terms of SNR and the
164 absolute T2m anomalies in ERA5, as compared with Figure 32. There is a good correspondence in all continents,
165 including parts of Europe (Fig. 4Fig. 5 c,d). The only difference between the two Figures is that they show the
166 results from re-forecasts with different initialization dates. Both target the boreal summer months (June-August),
167 but Figure 2Figure 3 shows the results from the May initialization while Figure 54 shows the results from the June
168 initialization. Similar qualitative conclusions can be made for precipitation (not shown).

169
170 In Figure 5Figure 6 we use the same methodology to sample years based on T2m SNR, but applied to specific
171 northern hemisphere mid-latitude regions: the Mediterranean, North and Central Europe, north western Asia, east
172 Asia, western North America and eastern North America. All the three skill metrics computed show that sampling
173 the 18 years with highest SNR, generally results in more skillful T2m predictions than when sampling all 24 years
174 or the 18 years with lowest SNR. The only exceptions are observed in North and Central Europe, where there is
175 basically no skill, as well as in eastern North America, where all the three selection methods show similar skill
176 levels. Examples of successful prediction of extreme (high) T2m years and high SNR are 1999 and 2003 in the
177 Mediterranean, 2002 in Northern/Central Europe, 1998 in northwestern Asia, 2006 and 1998 in western and
178 eastern North America, respectively. There are also some examples of extreme (high) T2m and low SNR, such as
179 2012 in the Mediterranean, or 1994 and 2016 in East Asia. However, higher overall GSS for the top T2m positive
180 anomalies indicates that on average, sampling years with high SNR results in better prediction of the extreme
181 events.

182
183 A similar analysis on precipitation is shown in Figure 6Figure 7. The results of precipitation qualitatively agree
184 with those of T2m. Precipitation skill is highest for years with highest SNR and lowest for years with lowest SNR,
185 the only exception being North and Central Europe, again a region with no skill in either precipitation or T2m
186 predictions. Years of successful predictions of low precipitation and high SNR are 1994 and 2000 in the
187 Mediterranean, 2015 in Northern/Central Europe, 1997 and 2001 in East Asia, 2003 in western North America,
188 and 2011 in eastern North America. Similar to T2m, GSS for low precipitation summers is generally higher for
189 the top 18 years (in terms of SNR) than for the bottom 18 years or for all 24 years. It is worth noting that skill
190 scores for precipitation are generally lower than those of T2m. This is primarily due to the lower overall
191 predictability of precipitation compared to T2m. Overall precipitation predictability is lower than T2m
192 predictability in the regions analyzed, since skill scores for precipitation are generally lower than those of T2m.
193 Note also that the same conclusions are obtained for both T2m and precipitation when separately sampling only
194 the half of years with highest and lowest SNRs and/or when varying the threshold to define the most extreme
195 years used in the GSS calculations (not shown).

196
197

198



199

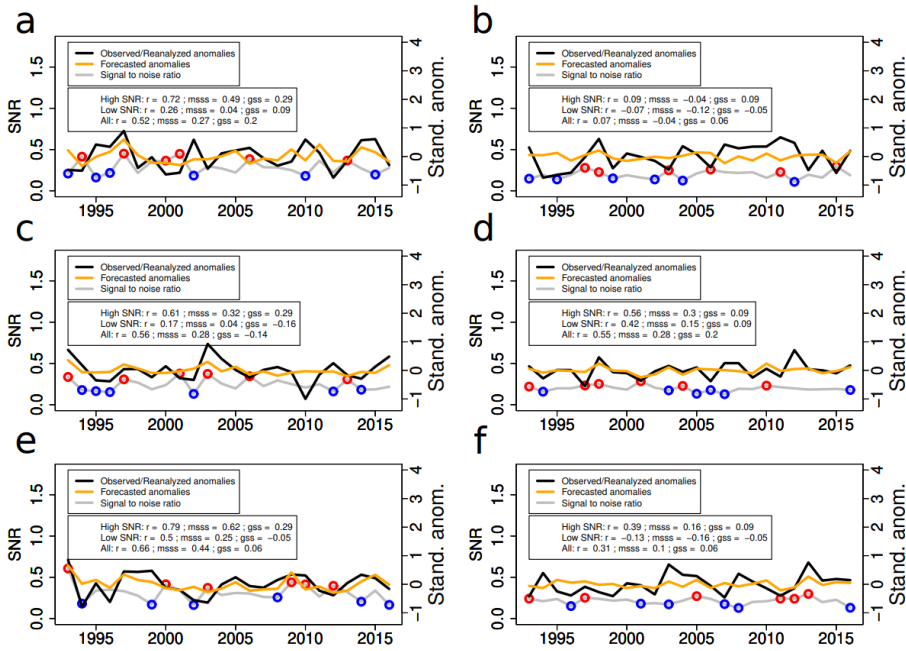
200

201

Figure 6: Area-averaged time series of observed and predicted, detrended and standardized mean summer T2m (right axis) and SNR (left axis) in (a) the Mediterranean (10W-35E, 30-45N), (b) North and Central Europe (10W-

202 35E, 45-65N), (c) northwestern Asia (35-70E, 40-65N), (d) East Asia (90-130E, 25-45N), (e) western North America
 203 (123-100W, 30-50N) and (f) eastern North America (90-70W, 30-55N). Skill metrics are provided separately for the 18
 204 years with highest SNR (excluding blue circles), the 18 years with the lowest SNR (excluding red circles) and for all 24
 205 years. The skill metrics are linear correlation, mean square skill score and Gilbert skill score (See methods). The p-
 206 values of the linear correlation coefficients are also displayed for each region. The values results are taken from the re-
 207 forecasts initialized in June.

208



209

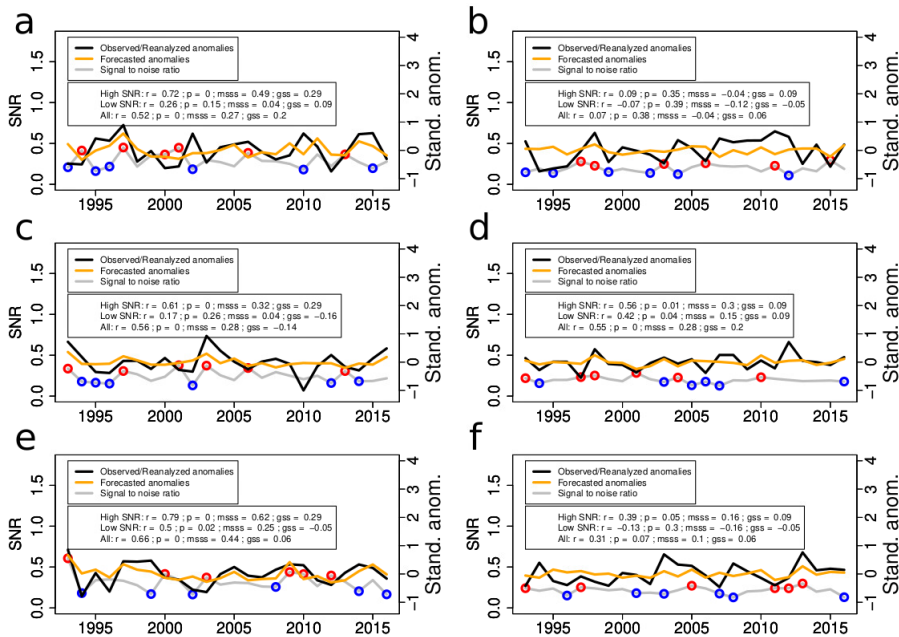


Figure 7: The same as Figure 6, but for precipitation.

4. Discussion

The SNR measures the relative weight of the ensemble mean anomalies with respect to the ensemble coherence. Its close resemblance in terms of spatial patterns with a skill metric like ACC indicates that it can provide complementary information related to seasonal climate predictability. We have shown that in regions where the forecasts are skilful, years with high SNR exhibit on average larger observed deviations from the mean than years with low SNR, for both for T2m and precipitation. This means that forecast systems are on average more reliable at predicting extremes when there is a higher coherence—excluding years with low SNR. This has been further demonstrated for several Northern Hemisphere mid-latitude regions during boreal summer. Ensemble coherence is also a good indicator of T2m and precipitation predictability, although appears to be only suitable for tropical and subtropical locations.

Despite the well known limitations of climate forecast systems (e.g. the signal to noise paradox), we have shown that in a multi-system ensemble, the SNR may provide valuable information as it represents an intrinsic measure of reliability for T2m and precipitation forecast. The short span of 24 years defining the common hindcast period is a limitation of this study. Hence, longer hindcasts would be necessary to obtain more robust results, but are currently unavailable for most of the multiple systems analyzed.

233

234 **References**

235

236 Acosta Navarro, J. C., García-Serrano, J., Lapin, V., [&and](#) Ortega, P. (2022). Added value of assimilating
237 springtime Arctic sea ice concentration in summer-fall climate predictions. *Environmental Research Letters*,
238 17(6), 064008.

239 Baehr, J., Fröhlich, K., Botzet, M., Domeisen, D. I., Kornbluh, L., Notz, D. [&and](#) Müller, W. A. (2015). The
240 prediction of surface temperature in the new seasonal prediction system based on the MPI-ESM coupled climate
241 model. *Climate Dynamics*, 44(9), 2723-2735.

242 Below, R., Grover-Kopec, E., [&and](#) Dilley, M. (2007). Documenting drought-related disasters: A global
243 reassessment. *The Journal of Environment & Development*, 16(3), 328-344.

244 Batté L., L. Dorel, C. Ardilouze, and J.-F. Guérémy, 202147: Documentation of the METEO- FRANCE
245 seasonal forecasting system 8. Météo-France, 36 pp., <https://www.umr-cnrm.fr/IMG/pdf/system8-technical.pdf>.

246 Bevacqua, E., Zappa, G., Lehner, F., [&and](#) Zscheischler, J. (2022). Precipitation trends determine future
247 occurrences of compound hot–dry events. *Nature Climate Change*, 12(4), 350-355.

248 Buontempo, C., Hanlon, H. M., Soares, M. B., Christel, I., Soubeyroux, J. M., Viel, C. [&and](#) Liggins, F. (2018).
249 What have we learnt from EUPORIAS climate service prototypes?. *Climate Services*, 9, 21 -32.

250 Doi T, Nonaka M and Behera S (2022). Can signal-to-noise ratio indicate prediction skill? Based on skill
251 assessment of 1-month lead prediction of monthly temperature anomaly over Japan. *Front. Clim.* 4:887782. doi:
252 10.3389/fclim.2022.887782

253 Ceglar, A., [&and](#) Toreti, A. (2021). Seasonal climate forecast can inform the European agricultural sector well
254 in advance of harvesting. *npj Climate and Atmospheric Science*, 4(1), 1 -8.

255 Eade, R. et al. Do seasonal to decadal climate predictions underestimate the predictability of the real world?
256 *Geophys. Res. Lett.* **41**, 5620–5628 (2014).

257 Enenkel, M., Brown, M. E., Vogt, J. V., McCarty, J. L., Reid Bell, A., Guha-Sapir, D. [&and](#) Vinck, P. (2020).
258 Why predict climate hazards if we need to understand impacts? Putting humans back into the drought equation.
259 *Climatic Change*, 162(3), 1161-1176.

260 Gualdi, S., A. Sanna, A. Borrelli, A. Cantelli, M. del Mar Chaves Montero, S. Tibaldi, 2020: The new CMCC
261 Operational Seasonal Prediction System SPS3.5. Centro Euro-Mediterraneo sui Cambiamenti Climatici. CMCC
262 Tech. Note RP0288, 26pp.

263 Hagedorn, R., Doblas-Reyes, F. J., [&and](#) Palmer, T. N. (2005). The rationale behind the success of multi-model
264 ensembles in seasonal forecasting—I. Basic concept. *Tellus A: Dynamic Meteorology and Oceanography*, 57(3),
265 219-233.

266 Hersbach, H., Bell, B., Berrisford, P., Hirahara, S., Horányi, A., Muñoz-Sabater, J. [&and](#) Thépaut, J. N. (2020).
267 The ERA5 global reanalysis. *Quarterly Journal of the Royal Meteorological Society*, 146(730), 1999 -2049.

268 Johnson, S. J., Stockdale, T. N., Ferranti, L., Balmaseda, M. A., Molteni, F., Magnusson, L., [&and](#) Monge-Sanz,
269 B. M. (2019). SEAS5: the new ECMWF seasonal forecast system. *Geoscientific Model Development*, 12(3),
270 1087-1117.

271 Lenssen, N. J., Goddard, L., [&and](#) Mason, S. (2020). Seasonal forecast skill of ENSO teleconnection maps.
272 *Weather and Forecasting*, 35(6), 2387-2406.

Field Code Changed

Formatted

273 MacLachlan, C., Arribas, A., Peterson, K. A., Maidens, A., Fereday, D., Scaife, A. A. & Madec, G. (2015).
274 Global Seasonal forecast system version 5 (GloSea5): A high-resolution seasonal forecast system. Quarterly
275 Journal of the Royal Meteorological Society, 141(689), 1072-1084.

276 Meehl, G. A., Richter, J. H., Teng, H., Capotondi, A., Cobb, K., Doblas-Reyes, F. & Xie, S. P. (2021).
277 Initialized Earth System prediction from subseasonal to decadal timescales. Nature Reviews Earth &
278 Environment, 2(5), 340-357.

279 Merryfield, W. J., Baehr, J., Batté, L., Becker, E. J., Butler, A. H., Coelho, C. A. & Yeager, S. (2020). Current
280 and emerging developments in subseasonal to decadal prediction. Bulletin of the American Meteorological
281 Society, 101(6), E869-E896.

282 Mishra, A. K., & Singh, V. P. (2010). A review of drought concepts. Journal of hydrology, 391(1-2), 202-
283 216.

284 Mishra, N., Prodhomme, C., & Guemas, V. (2019). Multi-model skill assessment of seasonal temperature and
285 precipitation forecasts over Europe. Climate Dynamics, 52(7), 4207-4225.

286 Murphy, A. H. (1988). Skill scores based on the mean square error and their relationships to the correlation
287 coefficient. Monthly weather review, 116(12), 2417-2424.

288 Scaife, A.A., Smith, D. A signal-to-noise paradox in climate science. npj Clim Atmos Sci 1, 28 (2018).
289 <https://doi.org/10.1038/s41612-018-0038-4>.

290 Smith, D.M., Scaife, A.A., Eade, R. et al. North Atlantic climate far more predictable than models imply. Nature
291 583, 796–800 (2020). <https://doi.org/10.1038/s41586-020-2525-0>.

292 Schneider, U., Becker, A., Finger, P., Meyer-Christoffer, A., Rudolf, B., & Ziese, M. (2011). GPCP Full Data
293 Reanalysis Version 6.0 at 1.0°: Monthly Land-Surface Precipitation from Rain-Gauges built on GTS-based and
294 Historic Data.

295 Toreti, A., Belward, A., Perez-Dominguez, I., Naumann, G., Luterbacher, J., Cronie, O. & Zampieri, M.
296 (2019). The exceptional 2018 European water seesaw calls for action on adaptation. Earth's Future, 7(6), 652-663.

297 Yin, J., Gentile, P., Slater, L., Gu, L., Pokhrel, Y., Hanasaki, N. & Schlenker, W. (2023). Future socio-
298 ecosystem productivity threatened by compound drought–heatwave events. Nature Sustainability, 1-14.

299 World Meteorological Organization (WMO, 2014). Forecast verification for the African severe weather
300 forecasting demonstration projects; No. 1132. Geneva, Switzerland: World Meteorological Organization.

301

Formatted: English (United States)